The Gyroid: A New Equilibrium Morphology in Weakly Segregated Diblock Copolymers

Damian A. Hajduk, Paul E. Harper, and Sol M. Gruner*

Department of Physics, Princeton University, Princeton, New Jersey 08544

Christian C. Honeker, Gia Kim,† and Edwin L. Thomas*

Department of Materials Science and Engineering, Massachusetts Institute of Technology, Cambridge, Massachusetts 02139

Lewis J. Fetters

Exxon Research and Engineering Company, Corporate Research Science Lab, Clinton Township, Annandale, New Jersey 08801

Received December 20, 1993; Revised Manuscript Received April 1, 1994®

ABSTRACT: We report the identification of a new equilibrium microdomain morphology in an intermediate to weakly segregated diblock copolymer melt. A polystyrene–polyisoprene (SI) diblock copolymer consisting of 37 wt % styrene and of total M_w = 27 400 was observed to transform from the lamellar morphology (in equilibrium at low annealing temperatures) to a new morphology at annealing temperatures approximately 50 °C below the order–disorder transition (ODT). The transformation was observed to be thermoreversible. Investigation of the new morphology via small-angle X-ray scattering (SAXS) and transmission electron microscopy (TEM) revealed the new structure to have remarkable three-dimensional long-range order, to belong to the cubic space group *Ia*3*d*, and to possess a bicontinuous cubic microstructure. From computer simulations of model structures and comparison with microscopy results, we propose models for the new morphology based on the triply periodic *G* minimal surface (gyroid) discovered by Schoen;[1] similar morphologies have been observed in a variety of microphase-separated surfactant–water systems. Blends of this diblock with various short-chain homopolymers were used to investigate the compositional extent of the region of *Ia*3*d* stability on the phase diagram; the results indicate that the *Ia*3*d* phase is stable over a wide range of minority component volume fractions.

Introduction

Under appropriate conditions, melts of AB diblock copolymers form microphase-separated structures in which domains consisting primarily of one block are locally separated from domains consisting primarily of the other block by an interfacial region. Early experiments observed, and early theories predicted, the existence of three stable ordered morphologies in both the weak and strong segregation limits: alternating lamellae of A and B, hexagonally packed cylinders of A in a matrix of B, and spheres of A in a matrix of B; subsequent experimental work established the packing of the spheres in the third morphology as body centered cubic (bcc). An excellent review of early theoretical and experimental work has been provided by Bates and Fredrickson.[2] In 1986, Thomas and co-workers identified a fourth equilibrium morphology, the ordered bicontinuous double diamond (OBDD), in a strongly segregated melt;[3] the new structure has since been observed in a variety of block copolymer systems.[4–6] Recently, Olmsted and Milner[7] have developed methods for calculating the free energy of bicontinuous morphologies in the strong segregation limit. A variety of new structures not predicted by the early theories have been observed in the weak segregation regime, including the lamellar-catenoid,[8,9] hexagonally modulated lamellae, and hexagonally packed lamellae.[10]

As part of a study on block copolymer thermal behavior, Gobran[11] observed an unusual microphase-separated morphology in a polystyrene–polyisoprene (SI) diblock copolymer. After casting from toluene, the sample formed a lamellar phase; upon heating to temperatures above 120 °C, diffraction characteristic of the lamellar structure vanished and a new set of peaks, appearing at spacing ratios of $\sqrt{3}$:$\sqrt{4}$, were observed. Examination of the high-temperature structure via transmission electron microscopy (TEM) of rapidly quenched specimens revealed the new morphology to consist of continuous, interpenetrating styrene and isoprene domains similar to those observed previously for the OBDD morphology. Unfortunately, the limited quality of the X-ray diffraction and TEM resulting from the restricted long-range order in the sample prevented definitive identification of the high-temperature phase at that time.

With long annealing treatments we have significantly improved the long-range order in the sample and have used small-angle X-ray scattering (SAXS) and TEM to determine the equilibrium microphase of this diblock as a function of temperature. The symmetry of the high-temperature morphology observed by Gobran has now been identified; these measurements demonstrate that the new structure is a bicontinuous cubic phase but *not* the OBDD morphology. Blends of the original diblock copolymer with various short-chain homopolymers have also been prepared and used to estimate the size of the region on the SI diblock phase diagram occupied by the high-temperature morphology. The results suggest that the new structure is stable over a reasonably broad range of composition which separates the lamellar and cylindrical morphologies.

Materials and Methods

The SI diblock copolymer used in this study was synthesized using a high-vacuum anionic polymerization technique previously described by Morton and Fetters;[12] details of the procedures used in characterizing this copolymer appear in Gobran.[11] Size-exclusion chromatography (SEC) yields weight-average molecular

* To whom correspondence should be addressed.
† Current address: Polaroid Corp., Waltham, MA 02154.
® Abstract published in *Advance ACS Abstracts,* June 1, 1994.

0024-9297/94/2227-4063$04.50/0

Table 1. Characteristics of the S and I Blocks[a]

block	M_w	$\langle R_0^2\rangle/M_w$ (Å^2 g^{-1} mol)	$\langle R_0^2\rangle^{1/2}$ (Å)	ρ (120 °C) (g/cm^3)	ϕ (120 °C)
S	10 100	0.434[32]	67	1.00[32]	0.33
I	17 300	0.616[31]	103	0.84[31]	0.67

[a] M_w = weight-average molecular weight of each block. R_0 = root-mean-square end-to-end distance of the appropriate homopolymer with the same number-average molecular weight. ρ = homopolymer density at 120 °C (at this temperature, the lamellar phase obtained upon casting transforms into the gyroid* morphology over 5 h). ϕ = volume fraction of each block in the copolymer at 120 °C.

weight (M_w) values of 10 100 (S block) and 27 400 (entire copolymer), giving a minority component weight fraction of 0.37. From the known densities of polystyrene and polyisoprene at 120 °C, the minority component volume fraction is estimated to be 0.33 at that temperature. The fraction of 3,4 units in the isoprene block (determined by ^{1}H NMR) is 6%. Table 1 summarizes the characteristics of the polymer. GPC calibration-grade homopolystyrene, M_w 760, M_w/M_n = 1.3, and calibration-grade homopolyisoprene, M_w 650, M_w/M_n = 1.13, were obtained from Polysciences (Fort Warrington, PA) and used without further purification.

Using values for χ obtained by Hashimoto et al.[13] and estimating N from the measured molecular weights of the blocks and the known molecular weights of the constituent monomers, $N\chi$ values for this system range from 22.4 at 90 °C to 16.4 at 160 °C. Density functional theory (a mean-field approach without fluctuation effects) predicts an upper bound for the weak segregation limit for f = 0.34 at $N\chi$ = 16,[14] suggesting that the copolymer is in the weak to early intermediate segregation regimes over the temperature range investigated.

Films of this material were prepared by casting from a solution of 10 wt % in toluene onto a deionized water surface. In contrast to conventional casting techniques which use a solid casting substrate, use of water minimizes deformation of the resulting (soft) film upon removal of the film from the casting vessel. Evaporation of the solvent took place over several days and produced a film of approximately 1-mm thickness. At this point, the film was removed from the casting vessel and dried under vacuum at 20 °C for 24 h. Samples approximately 2 × 4 mm in area were cut from the film at room temperature, mounted between thin mica sheets (for ease in handling), and used in subsequent experiments.

X-ray diffraction was used to determine the space group symmetry, lattice dimensions, and annealing behavior of polymer samples. Cu Kα X-rays were generated from a Rigaku RU-200BH rotating-anode X-ray machine equipped with a 0.2 × 2 mm microfocus cathode and Franks mirror optics. Samples were placed inside an evacuated sample chamber and maintained at the temperature of interest by a pair of thermoelectric devices (temperature range 0–185 °C, control accuracy ±50 mK). SEC performed on selected samples after prolonged annealing at high temperatures matched traces obtained from the polymer immediately after synthesis, demonstrating that the annealing protocols used did not produce measurable thermal degradation of the material. Two-dimensional diffraction images were collected with an image-intensified area detector designed around a Thomson CCD chip.[15] The sensitivity of the detector and the intensity of the beam line allowed collection of 2D diffraction patterns with typical exposure times of 10 min. After collection, images were digitized, corrected for detector response characteristics, and then written to magnetic tape. Images were then integrated azimuthally along an arc ±15° from the axis normal to the polymer film surface. X-ray diffraction from lamellar phases was characterized by diffraction peaks spaced at ratios of 1:2:3:4:... in reciprocal space; typically, only the first two orders were observed in short exposures. The third-order peak is suppressed in this material by the structure factor for scattering from lamellae of this minority component volume fraction; the fourth-order reflection was observed in long-time exposures (at least 900 s) of samples annealed for at least 2 h at 90 °C. X-ray diffraction from cylindrical phases was characterized by diffraction peaks spaced at ratios of $1:\sqrt{4}:\sqrt{7}$ in reciprocal space; the $\sqrt{3}$ reflection is suppressed by the structure factor for scattering from cylinders of the appropriate minority component volume fraction. X-ray diffraction from structures of cubic symmetry was characterized by the presence of peaks at different spacing ratios and will be discussed in subsequent sections.

The cubic nature of the high-temperature morphology was verified through birefringence measurements. Qualitative measurements were carried out on samples quenched from the low-temperature lamellar state and the high-temperature unknown state. Materials possessing cubic symmetry behave optically as an isotropic medium and thus have a zero birefringence; noncubic phases are optically anisotropic and therefore possess nonzero birefringences.

To confirm preliminary microdomain structure assignments made by X-ray diffraction and to determine the microphase geometry of the new cubic structure, transmission electron microscopy (TEM) was performed on selected X-ray samples. After annealing under vacuum on the X-ray line or in an annealing oven at prescribed temperatures for various times, certain samples were quenched to low temperatures in liquid nitrogen. Once quenched, the sample morphology is metastable at room temperature. Diffraction from quenched samples revealed no quantitative change in scattering pattern other than an increase in repeat spacings, thus permitting direct structural investigation of the high-temperature microdomain geometry. Quenched samples were microtomed at −110 °C with a Reichert-Jung FC 4E Microtome using a diamond knife. To provide image contrast, thin microtomed sections were exposed to OsO_4 vapors for 2–4 h. The sections of 500–1000-Å thickness were examined using the bright-field mode at 200 kV in a JEOL 200CX electron microscope. Tilt series were obtained using a goniometer stage with ±45° tilt capability and 360° rotation capability.

Selected regions of TEM prints were digitized at 300 dpi (dots per inch). Image sizes were 1024 × 1024 pixels and contained about 10–15 unit cells per edge. A two-dimensional fast Fourier transform (FFT) was then performed to quantify the degree of symmetry of the image.[16] Subsequent Fourier indexing of the transformed image permitted determination of the unit cell orientation in real space.

Computer simulations of various ordered bicontinuous structures based on the *Pn*3*m* and *Ia*3*d* space groups were used in combination with TEM images to identify the unknown three-dimensional microdomain morphology; the former space group is that of the OBDD morphology. The minority and majority components were assigned electron density values of 0 and 1, respectively. Starting from either Schwarz's D minimal surface[17] (for *Pn*3*m*/OBDD) or Schoen's G minimal surface[1] (for *Ia*3*d*), the majority component domains were modeled by adding layers of uniform thickness (measured normal to the minimal surface) to both sides of the minimal surface to yield a majority component volume fraction of 0.67. The channels in the resulting structure were filled by the minority component. This procedure produces a constant-thickness (CT) majority component domain which has been shown,[18] in the case of the Schwarz D surface, to approximate a corresponding member of the class of constant mean curvature (CMC) D surface structures discovered by Anderson.[19] For a volume fraction of 0.33, this approach permits both the prediction of X-ray reflection intensities and simulation of TEM images. The approximation of a CMC surface by a CT surface is expected to remain valid for the G surface CT structure as well at this volume fraction.

After creation of the CT structure, the model unit cell was Fourier transformed. The first 12 nonzero Fourier coefficients were used to express the electron density of the structure in terms of a Fourier series. Truncation of the series after 12 terms usually provides sufficient resolution for comparison with SAXS data as diffraction from cubic morphologies in other microstructured fluids usually exhibits at most 12 reflections. TEM projections were then obtained by integrating the electron density along the appropriate incident beam direction. For comparison with measured peak intensities obtained via SAXS, Fourier amplitudes for both the (constant-thickness) OBDD and *Ia*3*d* structures were squared, Lorentz-corrected,[20] and normalized by the resulting predicted intensity of the $\sqrt{3}$ reflection. Model calculations were performed using Mathematica 2.1 (Wolfram Research, Champaign, IL); further details on this procedure may be found in Harper.[21]

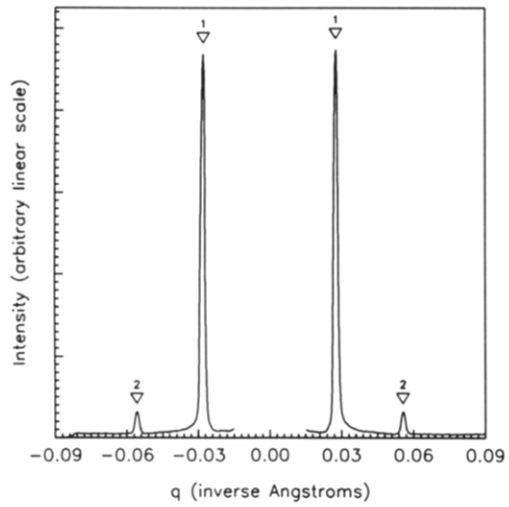

Figure 1. One-dimensional scattering profile of diffraction from a pure diblock film, annealed for 2 h at 90 °C. The profile was prepared from the two-dimensional diffraction image by integrating the total number of counts at a given distance from the center of the image over a 15° half-angle about the horizontal axis of the image. q is defined as $(4\pi/\lambda)\sin\theta$, where 2θ is the angle between the incident and scattered radiation and λ is the wavelength of the incident X-rays. 1 and 2 denote the expected peak positions for the first two reflections from a lamellar morphology; the repeat spacing (d) of this lattice is approximately 226 Å.

Results

Films of the pure diblock cast from toluene display a lamellar morphology when examined by X-ray diffraction at 20 °C. Two Bragg reflections at reciprocal space ratios of 1:2 are visible after only 180 s of integration; an additional reflection, corresponding to the fourth-order lamellar reflection, emerges from the background after considerably longer integration times (at least 900 s). As previously noted, the third-order lamellar reflection is suppressed by the structure factor for scattering from lamellae of the appropriate minority component volume fraction. The repeat spacing of the lattice is 200 ± 5 Å at 20 °C. After 2 h of annealing at 90 °C, the long-range order in the system increases (as evidenced by a decrease in peak widths) and the repeat spacing of the lattice increases to 226 ± 2 Å; see Figure 1. Films cast from hexane, a solvent which is strongly preferential for the isoprene block of the polymer, show only one (relatively broad) diffraction peak when examined with X-ray diffraction at 20 °C. Annealing such films for 2 h at 90 °C produces a lamellar morphology with X-ray reflections in the ratio of 1:2:4 and a repeat spacing of 218 ± 2 Å; the lattice spacing continues to increase with further annealing and eventually approaches the value of 226 Å obtained for films cast from toluene. Annealing pure diblock films at temperatures between 90 and 120 °C does not produce a change in morphology; the lamellar diffraction signature persists after isothermal annealing periods ranging from 1 to 100 h. Transmission electron micrographs of samples cast from toluene and subjected to such low-temperature annealing treatments show well-organized lamellae; see Figure 2. The dark osmium-stained isoprene phase appears wider than the lighter polystyrene domains in accordance with the known volume fraction and measured SAXS domain spacings.

Changes in morphology are observed after annealing at higher temperatures. After several hours of isothermal annealing at 120 °C, the second and fourth orders of the lamellar diffraction signature slowly decline in intensity and eventually disappear, while the intensity and width of the first-order reflection do not change (to within experimental error). At isothermal annealing temperatures above 120 °C, a new peak forms on the high-q side of the former lamellar first-order ring and grows to an intensity approximately 10% of that of the original peak (as was originally noted by Gobran[11]); see Figure 3. The two peaks appear at reciprocal space position ratios of $\sqrt{3}$:$\sqrt{4}$. As the annealing temperature increases, the rate at which this transformation occurs increases. Unambiguous identification of the new morphology is impossible with only two peaks: the observed peak position spacing ratio is consistent with allowed reflections from all of the known nonlamellar strong segregation morphologies, although the absence of peaks at spacing ratios of 1 (for hexagonally packed cylinders and bcc spheres) and $\sqrt{2}$ (for OBDD) strongly suggests that the scattering signal represents a new morphology. The $\sqrt{3}$:$\sqrt{4}$ signature persists up to approximately 160 °C; at this temperature, disordered regions begin to form in the sample as evidenced by the decline in intensity of both Bragg reflections and the simultaneous appearance of a diffuse scattering ring.

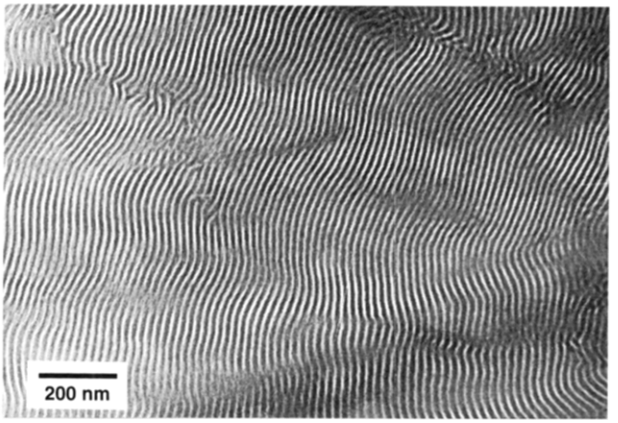

Figure 2. TEM micrograph of a sample of pure diblock cast from toluene and annealed for 1 week at 115 °C. Polyisoprene domains have been stained with OsO_4 to provide contrast and appear dark in the image. A well-ordered lamellar morphology with a repeat period of approximately 210 Å is clearly evident.

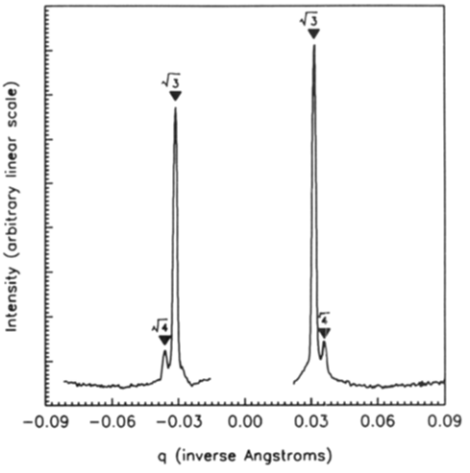

Figure 3. One-dimensional scattering profile obtained from a diblock film annealed for 1.7 h at 150 °C. Two peaks are observed, at a reciprocal space position ratio of $\sqrt{3}$:$\sqrt{4}$; as this position ratio is consistent with diffraction from several nonlamellar morphologies including the OBDD and cylindrical phases, the identity of the new structure cannot be determined from such diffraction alone. If the peak appearing at a spacing ratio of $\sqrt{3}$ is interpreted as a (111) reflection, the repeat spacing (d) of the new lattice is approximately 348 Å.

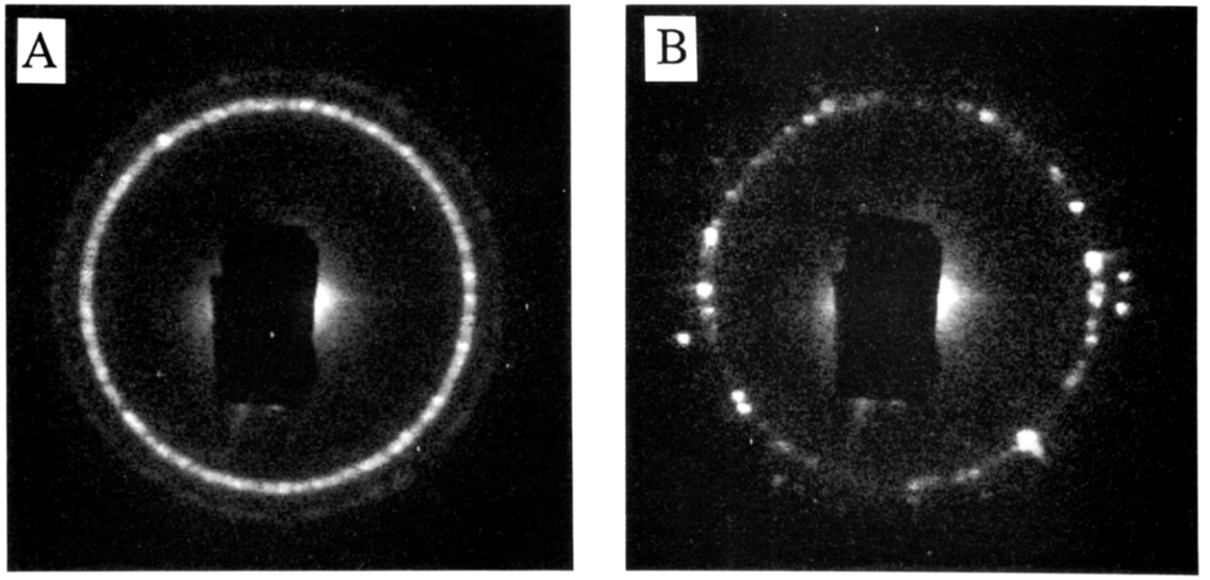

Figure 4. Two-dimensional diffraction images obtained from a diblock film immediately upon reaching an annealing temperature of 160 °C (image A) and after 3.0 h of annealing at that temperature (image B). The dark rectangular region at the center of the image is the shadow of the beam stop used to prevent the direct beam from striking the detector. The diffraction signature of the new morphology appears immediately upon reaching the annealing temperature; as isothermal annealing progresses, the nearly uniform rings of the original image begin to exhibit significant azimuthal anisotropy and eventually transform into a circular array of extremely bright spots. Such behavior would be produced by the annealing of a sample consisting of a large number of small, randomly oriented domains into one composed of a small number of large, highly ordered domains exhibiting long-range crystalline order. The reason for this transformation is unknown.

The rate of disordering increases with increasing annealing temperature, as expected: complete transformation of the sample from a microphase-separated morphology to an isotropic melt occurs in less than 1 h at 175 °C.

As the sample nears the order–disorder transition, the powder diffraction rings composing the $\sqrt{3}$:$\sqrt{4}$ signature begin to show significant azimuthal variation in scattered intensity. With further isothermal annealing at or above 160 °C, the powder rings evolve into a set of extremely bright diffraction spots located at the radial positions previously occupied by the smooth powder rings; see Figure 4. These spots are superimposed on a diffuse ring arising from scattering from disordered regions of the sample; sudden quenching of the sample to 150 °C or below causes the disappearance of the diffuse ring and the reappearance of the sharp powder rings characteristic of the new morphology while leaving the sharp diffraction spots unaffected. The radial and azimuthal dimensions of these spots appear to be limited by the optical characteristics of the X-ray apparatus, indicating that the sample now consists of a small number of large crystalline grains of the new morphology coexisting with disordered regions. Such well-oriented large grains are usually associated with more conventional crystals rather than the "soft" materials examined here. Indeed, TEM images of samples showing this diffraction signature reveal an unusual degree of long-range ordering with few grain boundaries, observations which are consistent with the X-ray images; see Figure 5. The TEM images show domain structures inconsistent with projections of either cylinders or various packings of spheres; it is not immediately apparent whether they are consistent with the OBDD morphology or not.

Observation of a sample of the pure diblock which was quenched from the high-temperature morphology exhibited nearly zero transmitted intensity when placed between crossed polarizers, indicating zero birefringence and hence an optically isotropic structure such as a cubic phase. For comparison, a polycrystalline SIS triblock copolymer known to possess a cylindrical S domain morphology was examined in the same manner and produced a nonzero birefringence characteristic of an optically anisotropic structure.

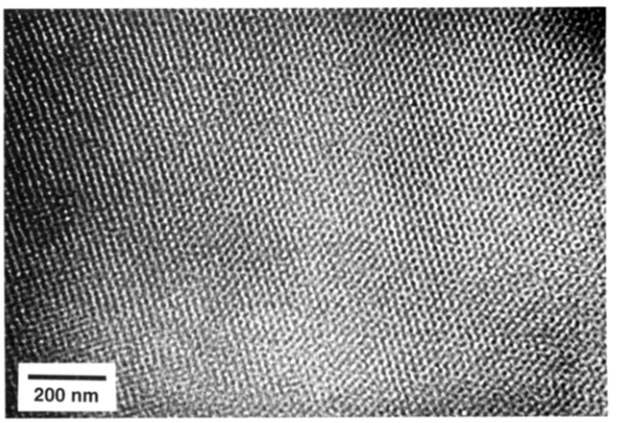

Figure 5. TEM micrograph of a sample of SI diblock annealed for 22 h at 160 °C followed by quenching in liquid nitrogen to preserve the high-temperature ordered morphology.

Attempts to obtain higher order X-ray reflections from samples exhibiting the powder $\sqrt{3}$:$\sqrt{4}$ signature by integrating for extremely long periods of time were unsuccessful when carried out at high temperatures. This failure may result from an absence of higher order Fourier components in the monomer concentration profile of the morphology; such a dominance of the concentration profile by the low-order terms in the series is expected for melts near the order–disorder transition temperature (i.e., in the weak segregation limit). Samples exhibiting this signature also failed to reveal any higher order components when quenched to 20 °C and examined there; these difficulties may arise from preservation of the high-temperature concentration profile by the quenching process. Similar measurements on samples exhibiting the large-grain $\sqrt{3}$:$\sqrt{4}$ signature (as shown in Figure 4B) also failed to produce higher order reflections; in addition to the reasons given above, this may be due to a failure to meet the Bragg diffraction condition given the orientations

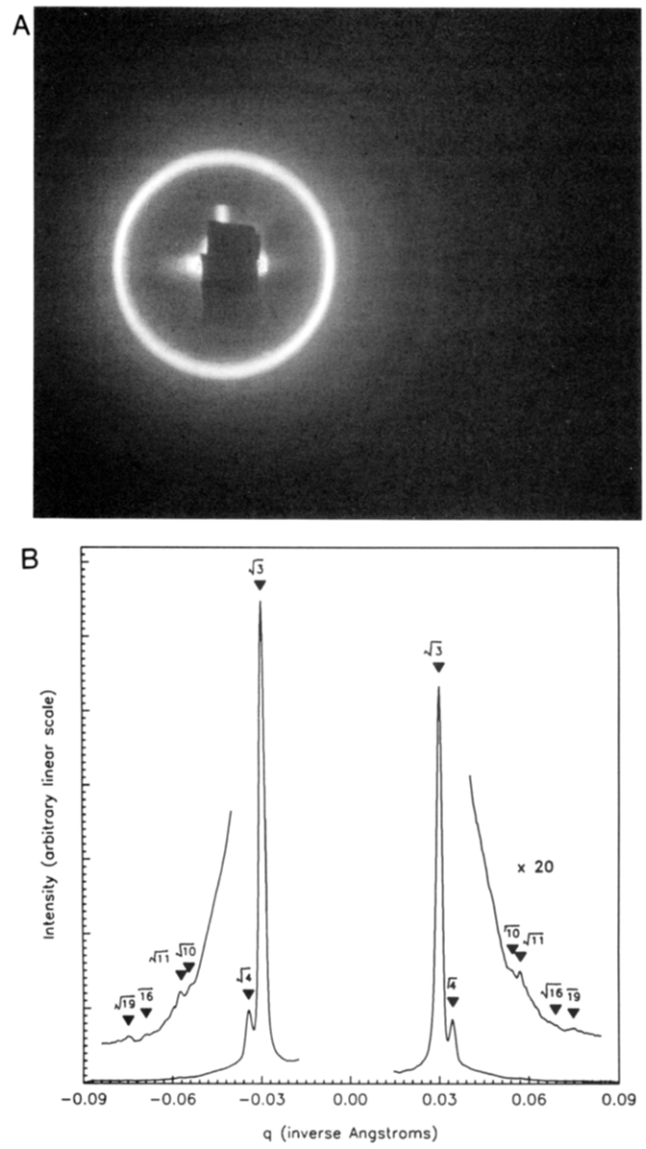

Figure 6. (A) Two-dimensional scattering image obtained from a pure diblock film annealed for 4 h at 150 °C to establish the new morphology, followed by quenching in liquid nitrogen and subsequent annealing at 120 °C for 4 h to eliminate disorder induced by quenching and increase the number of higher order Fourier components in the monomer concentration profile (as described in the text). This image was obtained after integrating for 8 h at 120 °C; comparison of diffraction before and after this period revealed no change in the scattering from the sample. (B) One-dimensional profile prepared from the two-dimensional image. $\sqrt{3}$, $\sqrt{4}$, $\sqrt{10}$, $\sqrt{11}$, $\sqrt{16}$, and $\sqrt{19}$ denote the position ratios of the observed reflections; as discussed in the text, such reflections are most consistent with a structure possessing *Ia*3*d* symmetry.

of the crystallites with respect to the incident X-ray beam. Fortunately, higher diffraction orders eventually appear in samples exhibiting both the powder and large-grain forms of the new high-temperature diffraction signature after several hours of isothermal annealing at 120 °C following the establishment of the new morphology. Thus, a treatment to obtain higher order reflections consists of 2 h of annealing at 150 °C (if powder rings are desired) or 12 h of annealing at 160 °C (if large grains are desired), followed by annealing at 120 °C. After 16 h of integration (an extremely long time for the SAXS equipment employed here), additional Bragg reflections are observed at reciprocal space position ratios of $\sqrt{10}$, $\sqrt{11}$, $\sqrt{16}$, and $\sqrt{19}$; see Figure 6.

Diffraction reflections at position ratios of $\sqrt{10}$, $\sqrt{11}$, and $\sqrt{19}$ are inconsistent with all noncubic space groups. Micrographs of the new structure show continuous regions of the minority (styrene) component (Figure 5), effectively eliminating any packings of spheres from consideration and suggesting a bicontinuous structure. A total of 3 of the 17 possible cubic extinction symbols (*P*..., which includes the *Pm*3*m* or primitive cubic space group; $P4_2..$; and *Pn*.., which includes the P*n*3*m* space group (OBDD)) have reflections at spacing ratios consistent with those observed for the new morphology. As can be seen from Table 2A, these symbols also possess a considerable number of additional reflections that do not appear in the diffraction from the new structure. The absence of high-order reflections could be attributed to paracrystalline (type II) disorder in the sample, but the observation of a reflection of reasonable width at a position ratio of $\sqrt{19}$ implies that reflections at lower position ratios are not washed out by this effect. If reflections at lower position ratios actually exist for the (unknown) microstructure in question, it is more likely that the corresponding terms in the Fourier transform of the electron density of the new structure possesses negligible amplitude. The absence of one or two low-order reflections could be explained by a minimum in the square of the structure factor of the new morphology, but such reasoning does not explain the absence of a large number of low-order reflections. In particular, the absence of the lowest-order diffraction peaks is difficult to explain as a result of structure factor cancellation. All of this evidence *suggests* that the new structure does not belong to one of these three space groups: we note, however, that we are presently unable to *prove* that this is the case.

Additional possibilities for the space group of the new morphology arise when the observed position ratios are reinterpreted as $\sqrt{6}$:$\sqrt{8}$:$\sqrt{20}$:$\sqrt{22}$$\sqrt{32}$:$\sqrt{38}$; since all of these values are divisible by $\sqrt{2}$, the observed spacings will appear at the ratios discussed earlier. Support for this hypothesis comes from comparison of unit cell spacings obtained from SAXS and TEM. SAXS data suggest a unit cell of approximately 350 Å (if the lowest order spacing is $\sqrt{3}$), while TEM observations suggest a unit cell of approximately 500 Å. While the sample preparation procedures for microscopy are known to slightly alter unit cell spacings, those effects cannot account for the enormous discrepancy mentioned here. The two observations become consistent if the lowest diffraction order is reinterpreted as $\sqrt{6}$, yielding a unit cell size of approximately 500 Å. Of the 17 possible cubic extinction symbols (or sets of permitted X-ray reflections), the first 12 (composing all of the cubic space groups with *P* and *I* symmetry) are consistent with the $\sqrt{6}$:$\sqrt{8}$:... reflections; see Table 2B. As before, the absence of a considerable number of reflections predicted for most of the extinction symbols effectively eliminates the corresponding space groups from consideration. The observed ratios appear most consistent with the *Ia.d* symbol, which corresponds to a structure with *Ia*3*d* symmetry and whose reflections appear at position ratios of $\sqrt{6}$:$\sqrt{8}$:$\sqrt{14}$$\sqrt{16}$:$\sqrt{20}$:$\sqrt{22}$:$\sqrt{24}$:$\sqrt{26}$: $\sqrt{30}$:$\sqrt{32}$:$\sqrt{38}$. As all of the theoretically predicted ratios are divisible by $\sqrt{2}$, the experimentally observable position ratios are $\sqrt{3}$:$\sqrt{4}$:$\sqrt{7}$:$\sqrt{8}$$\sqrt{10}$:$\sqrt{11}$:$\sqrt{12}$:$\sqrt{13}$: $\sqrt{15}$:$\sqrt{16}$:$\sqrt{19}$. Three-dimensional structures with *Ia*3*d* symmetry have been observed in other microphase-separated systems, such as suspensions of anionic soaps in water;[22] this observation represents the first identifica-

Table 2. Extinction Symbols Consistent with the Observed Reflection Spacing Ratios[36] and Ratios Multiplied by $\sqrt{2}$ (x Denotes Allowed Reflection; X Denotes Reflections Observed Experimentally)

A. Observed Reflection Spacing Ratios

square of modulus[a]	cubic extinction symbol			obsd reflctn	square of modulus[a]	cubic extinction symbol			obsd reflctn
	P...[b]	$P4_2$..	*Pn*..[c]			*P*...[b]	$P4_2$..	*Pn*..[c]	
1	x				11	X	X	X	X
2	x	x	x		12	x	x	x	
3	X	X	X	X	13	x	x		
4	X	X	X	X	14	x	x	x	
5	x	x			16	X	X	X	X
6	x	x	x		17	x	x	x	
8	x	x	x		18	x	x	x	
9	x	x	x		19	X	X	X	X
10	X	X	X	X					

B. Observed Reflection Spacing Ratios Multiplied by $\sqrt{2}$

square of modulus[a]	cubic space group extinction symbol												obsd reflctn
	P...[b]	$P4_2$..	$P4_1$..	*Pn*..[c]	*P..n*	*Pn.n*	*Pa.*	*I*...	$I4_1$..	*Ia.*	*I..d*	*Ia.d*	
1	x												
2	x	x	x	x	x	x		x	x				
3	x	x	x	x			x						
4	x	x		x	x	x	x	x		x			
5	x	x	x		x		x						
6	X	X	X	X	X	X	X	X	X	X	X	X	X
8	X	X	X	X	X	X	X	X	X	X	X	X	X
9	x	x	x	x			x						
10	x	x	x	x	x	x		x	x		x		
11	x	x	x	x			x						
12	x	x	x	x	x	x	x	x	x	x			
13	x	x	x		x		x						
14	x	x	x	x	x	x	x	x	x	x	x	x	
16	x	x	x	x	x	x	x	x	x	x	x	x	
17	x	x	x	x	x		x						
18	x	x	x	x	x	x	x	x	x	x			
19	x	x	x	x			x						
20	X	X	X	X	X	X	X	X	X	X	X	X	X
21	x	x	x	x	x	x	x						
22	X	X	X	X	X	X	X	X	X	X	X	X	X
24	x	x	x	x	x	x	x	x	x	x	x	x	
25	x	x	x		x		x						
26	x	x	x	x	x	x	x	x	x	x	x	x	
27	x	x	x	x	x	x	x						
29	x	x	x	x	x	x	x						
30	x	x	x	x	x	x	x	x	x	x	x	x	
32	X	X	X	X	X	X	X	X	X	X	X	X	X
33	x	x	x	x			x						
34	x	x	x	x	x	x	x	x	x	x	x		
35	x	x	x	x	x	x	x						
36	x	x	x	x	x	x	x	x	x	x			
37	x	x	x		x		x						
38	X	X	X	X	X	X	X	X	X	X	X	X	X

[a] Modulus m is defined for reflection (hkl) as $h^2 + k^2 + l^2 = m^2$. [b] Primitive cubic. [c] OBDD.

tion of this symmetry in block copolymer systems.[23] Again, we note that all of the allowed reflections for the *Ia*3*d* space group also appear in a number of other space groups. We are therefore unable to conclusively *prove* that the new structure has *Ia*3*d* symmetry.

Determination of the detailed microdomain structure from X-ray diffraction is often problematic. Although definitive identification of the microstructure from TEM data requires considerable effort (and will be deferred to a future publication), images of the new morphology agree reasonably well with computer-generated projections of a three-dimensional constant thickness structure based on Schoen's G surface (see Figures 7–9). The presence of both 3-fold and 4-fold projections signals a cubic phase. By using the goniometer stage, it is possible to select appropriately oriented grains. Figures 8 and 9 show images which can be indexed as [111] and [100] projections (respectively) by comparison of the strong allowed Fourier components for the projection in question with the power spectrum of the digitized image. Also shown in the figures are simulated projections based on the constant-thickness G surface structure. The data match to the model is quite remarkable both in Fourier space and real space. Accordingly, the new morphology is tentatively named "gyroid*" (the asterisk will be used to distinguish the experimentally observed morphology from Schoen's G surface, which has also been given the name "gyroid"). Many of the constant-thickness gyroid* projections resemble similar projections of the OBDD morphology. For example, the [111] projection of the OBDD, known as the "wagon wheel", is similar to the [111] projection of the gyroid* structure (as seen in Figure 8). Differentiation of the two morphologies via TEM therefore requires careful work. Fortunately, the SAXS data have already demonstrated that the *Pn*3*m* space group of the OBDD morphology is not present in this sample. Unequivocal assignment of an interfacial microstructure to the gyroid* phase would require Fourier inversion of the diffraction pattern, a procedure which is almost always practically impossible for complex diblock phases because of the

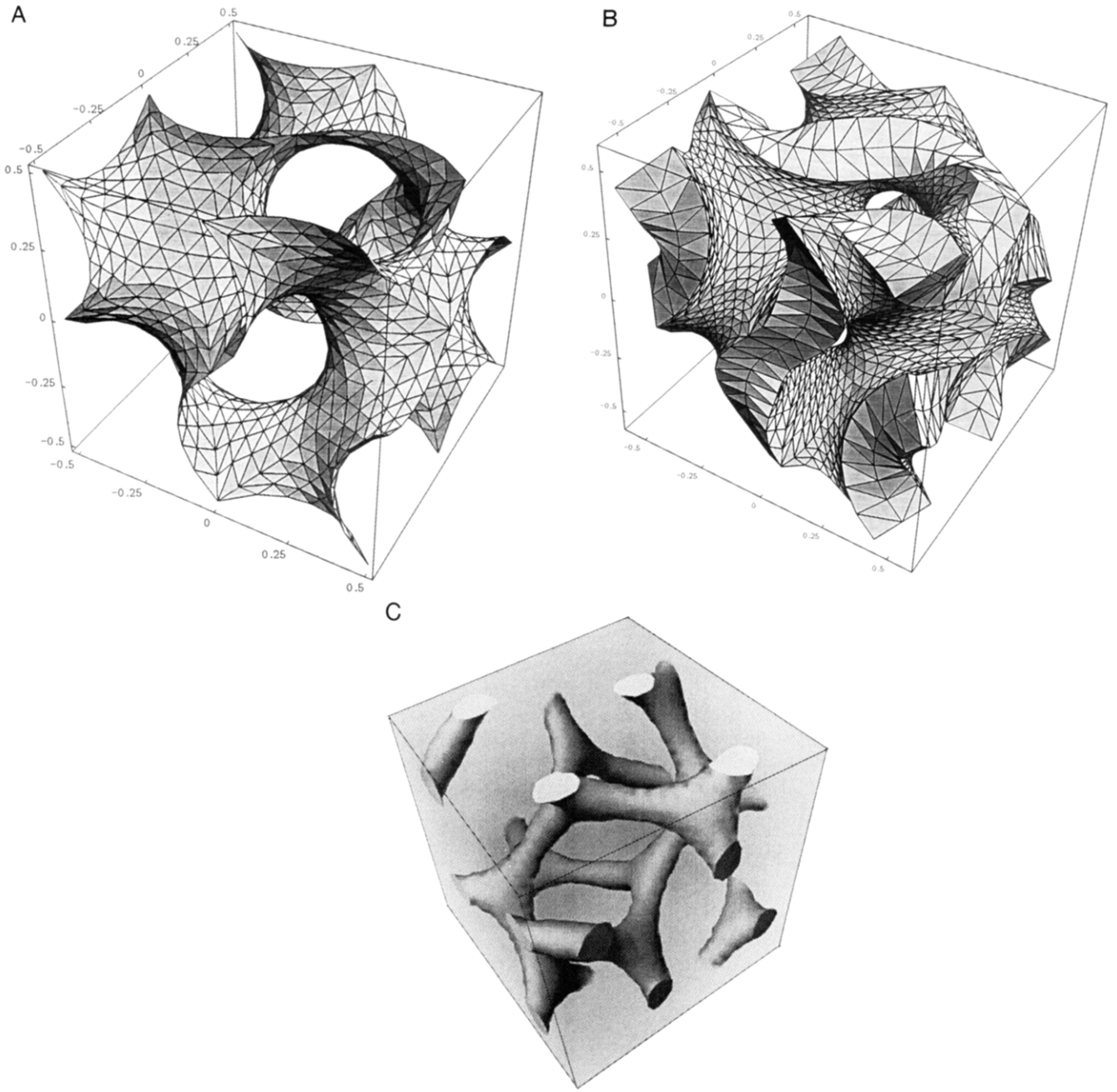

Figure 7. (A) Perspective view of the G surface having space group *Ia*3*d*. (B) A constant-thickness structure, based on the G surface, proposed as a possible model for the gyroid* morphology at a minority component volume fraction of 0.33. In order to Fourier transform the volume bounded by this surface, the surface was divided into a grid, each square of which was subdivided into two triangles. The grid shown here has edge lengths twice those actually used for calculation. (C) The channel structure (minority component domains) of the constant-thickness model for the gyroid* morphology shown in Figure 7B. Details of the construction of these models may be found in Harper.[21]

weakness of the higher diffraction orders.

Additional evidence in support of the assignment of *Ia*3*d* symmetry and constant-thickness gyroid* microstructure to the new morphology may be obtained from comparison of experimentally measured diffraction peak intensities to predicted values for the constant-thickness gyroid* and OBDD structures; see Table 3. All values have been normalized by the intensity of the $\sqrt{3}$ reflection. The constant-thickness model for the OBDD predicts a strong $\sqrt{2}$ which is not observed experimentally as well as reasonably strong reflections at $\sqrt{4}$, $\sqrt{6}$, and $\sqrt{12}$. Although a $\sqrt{4}$ reflection is observed , the absence of the other three peaks in the experimental data supports the claim that the new structure is not OBDD. The constant-thickness model for the gyroid* predicts strong reflections at $\sqrt{3}$ and $\sqrt{4}$ only. All other reflections are relatively weak, in agreement with experimental observations. Differences between the predicted and observed values for higher order peaks are difficult to measure due to the considerable uncertainty present in the experimental observations. Some differences are expected, however, as the experimental microstructure probably deviates from the assumed constant-thickness model.

Once the gyroid* phase has been fully established in a given specimen, subsequent isothermal annealing at temperatures below 120 °C leads to the reappearance of the lamellar morphology; see Figure 10A,B. Although SAXS indicates complete conversion of the initial lamellar structure to the gyroid* phase after brief annealing periods at high temperatures, transformation of the gyroid* phase

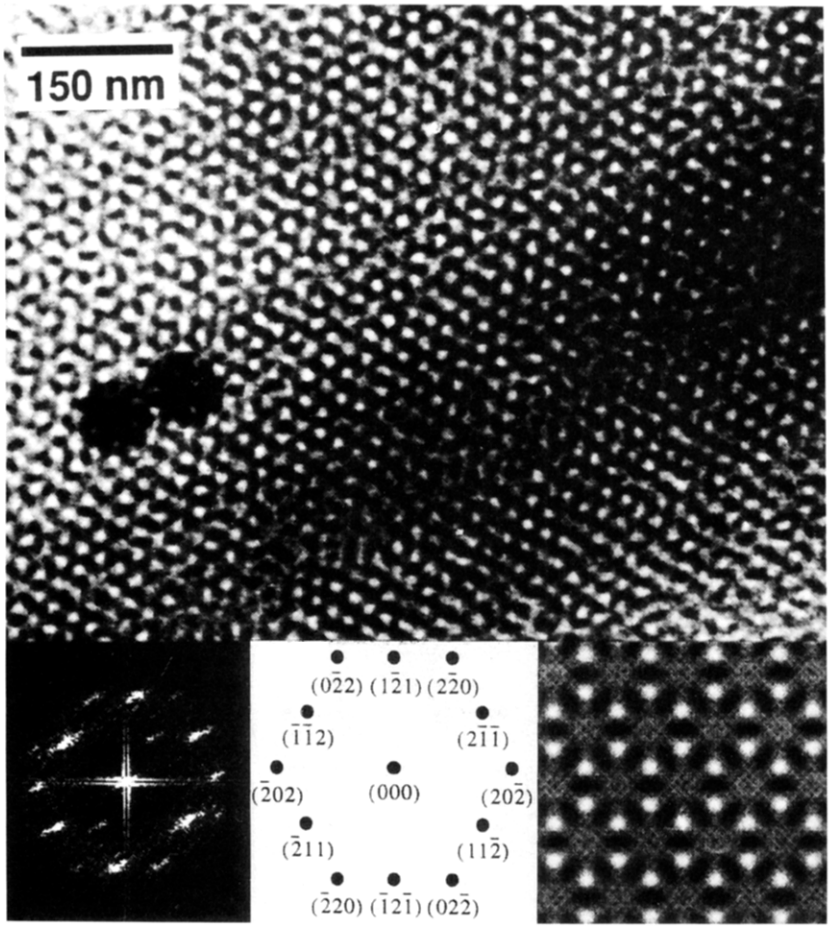

Figure 8. TEM micrograph of a different section of the SI diblock examined in Figure 5. The pattern shows approximately 3-fold symmetry corresponding to the [111] projection of the cubic structure. The insets show the image FFT and indexed diffraction pattern displaying six {211} and six {022} reflections with approximately 6-fold symmetry about the origin. The inset on the far right is a simulated [111] projection of the constant-thickness gyroid* structure. Minority component (styrene) domains appear white in both the micrograph and the simulation.

to the lamellar morphology at low temperatures is not complete. The cubic diffraction signature is observed in samples annealed for as long as 110 h at 110 °C, indicating that full reversibility of the transition from lamellae to gyroid* is kinetically limited. Diffraction rings obtained from the original lamellar morphology are azimuthally isotropic, indicating an absence of preferred orientation; rings obtained from the lamellar morphology which forms upon cooling from the gyroid* phase are strongly anisotropic, indicating an oriented morphology in which the lamellae stack preferentially in the plane of the film. The degree of orientation and the overall intensity of the lamellar diffraction decrease as the X-ray beam is moved away from the surface of the film into the bulk of the sample. As the lamellar morphology is one-dimensional, while the gyroid* morphology is three-dimensional, for long-range lamellar ordering to develop, the gyroid* symmetry of the high-temperature structure must be broken to create a preferred direction along which the lamellar normals can line up. Such symmetry breaking is provided by the surface of contact between the film and the mica sample holder. In the sample interior, small, randomly-oriented grains of lamellae are formed. Consequently, diffraction that arises from lamellar grains deep inside the sample is weak and lacks the higher orders essential for identification of the lamellar morphology.

Immediately after reaching the lower annealing temperature, the gyroid* phase spacing and lamellar spacing differ sufficiently that separate diffraction arising from both lattices can be observed. As annealing continues, however, the peaks of the gyroid* lattice shift so that the (211) reflection coincides with the first-order lamellar reflection, effectively obscuring the lamellar diffraction. The lamellar spacing changes by at most 1 Å during this time; subsequent annealing of the sample for periods as long as 24 h produces no further changes in either the lamellar or the gyroid* phase spacing. The reappearance of the original lamellar morphology demonstrates that the transition is thermally reversible and hence that the lamellar and gyroid* phases are in equilibrium at different temperatures in the pure diblock.

Further evidence for the equilibrium nature of the gyroid* phase comes from experiments on samples quenched from the disordered state. Diffraction taken from samples annealed for 1 h at 175 °C showed a single broad peak characteristic of an isotropic melt. After establishing the presence of the disordered phase, samples were quenched *in-situ* to a temperature of interest and annealed for 1 h before examination via SAXS. Typical quench times were less than 1 min. Samples examined at 150 °C, where the gyroid* phase is believed to be stable, produced diffraction reflections characteristic of this morphology at position ratios of $\sqrt{3}$:$\sqrt{4}$. Samples quenched to 100 °C, where the lamellar phase is believed to be stable, produced reflections at position ratios of 1:2. Occasionally, sharp reflections of low intensity were observed at position ratios of $\sqrt{3}$:$\sqrt{4}$ in these samples as well, indicating that a small amount of the gyroid* morphology formed in the sample during the passage

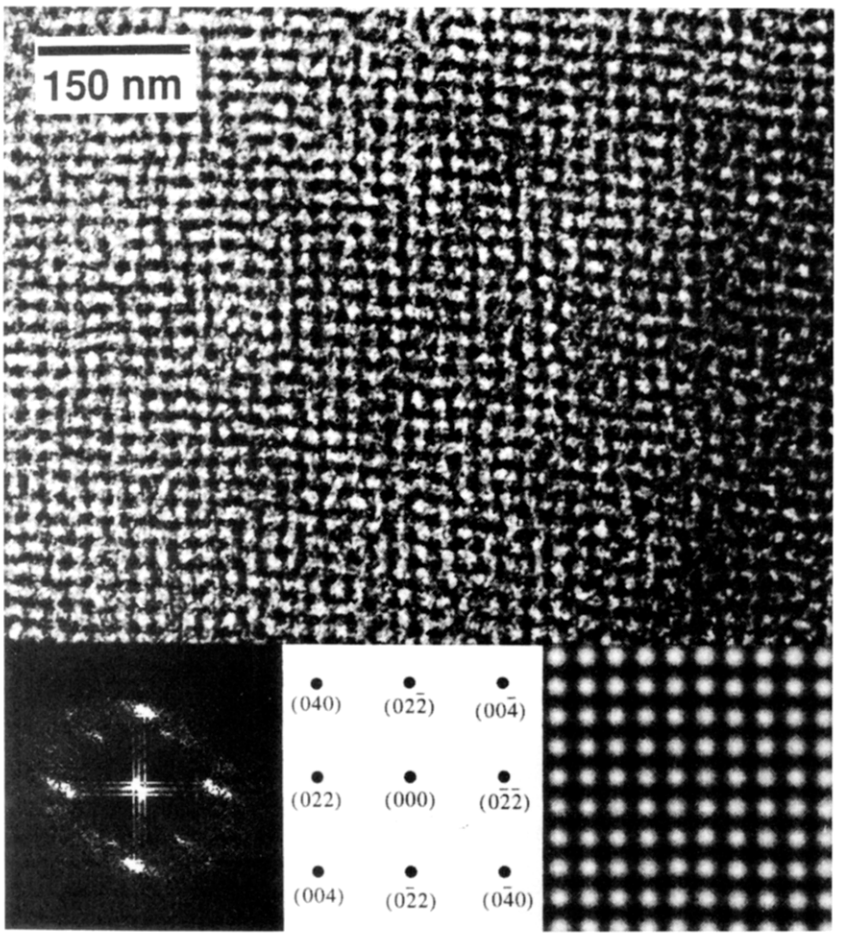

Figure 9. TEM micrograph of another region of the SI diblock examined in Figure 8. The pattern shows approximately 4-fold symmetry corresponding to the [100] projection of the cubic structure. The insets show the image FFT and indexed diffraction pattern, displaying four strong {022} reflections with approximately 4-fold symmetry about the origin. The inset on the far right shows a simulated [100] projection of the constant-thickness gyroid* structure.

Table 3. Comparison of Predicted and Measured Peak Intensities for 33 Vol % Minority Component[a]

square of modulus[b]	corresponding reflctns		predicted intens		measd intens
	OBDD	gyroid*	OBDD	gyroid*	
2	(110)	NA	2.837	NA	NO
3	(111)	(211)	1.000[c]	1.000[c]	1.000[c]
4	(200)	(220)	0.042	0.168	0.069
6	(211)	NA	0.013	NA	NO
7	NA	(321)	NA	0.002	NO
8	(220)	(400)	0.006	<0.001	NO
9	(221)	NA	0.038	NA	NO
10	(310)	(420)	0.020	0.001	0.001
11	(311)	(332)	0.006	0.008	0.002
12	(222)	(422)	0.038	0.006	NO
13	NA	(431)	NA	0.008	NO
14	(321)	NA	0.024	NA	NO
15	NA	(521)	NA	0.001	NO
16	(400)	(440)	0.004	<0.001	<0.001

[a] NA = not allowed. NO = not observed. [b] Modulus m is defined for reflection (hkl) as $h^2 + k^2 + l^2 = m^2$. Since all of the moduli for the observed reflections of the $Ia3d$ space group are divisible by $\sqrt{2}$, the experimentally observed reflections appear at the spacing ratios with respect to the position of the first order given in the table above. [c] All intensities have been normalized by the intensity of the $\sqrt{3}$ reflection as this is the lowest diffraction order that appears in the experimental data.

through the temperature range in which the cubic microstructure is stable. Since all samples started from the identical isotropic state, the formation of two different microstructures depending on the final annealing temperature provides further evidence that the gyroid* microstructure is an equilibrium morphology.

In an attempt to determine the compositional extent of the gyroid* phase region on the phase diagram, several films of diblock copolymer blended with homopolymer were prepared by casting from toluene onto water. In part, the inspiration for examination of such blends comes from previous experiments on phospholipid-water phase behavior.[24] Comparisons between a blend of known minority component volume fraction and a diblock of identical volume fraction are often inexact; a considerable body of recent experimental work has demonstrated that the addition of even slight amounts of homopolymer can have a considerable influence on phase behavior;[5,25,26] again, the analogy to lipid–water systems pertains.[24] While experimental evidence suggests that such effects may be minimized by the use of homopolymers of extremely low molecular weight, which presumably are distributed more uniformly throughout the domains of a given block, these effects are certainly not eliminated by this procedure. Moreover, SAXS is relatively insensitive to the presence of homopolymer domains which coexist with ordered microstructures, a situation which may exist in blends containing a significant fraction of homopolymer. Definitive measurement of the gyroid* region awaits the synthesis of a carefully controlled set of diblocks with a range of minority component volume fractions; the following results should therefore be interpreted as merely suggestive of the composition range over which the gyroid* structure appears.

Figure 11 depicts the morphology observed via SAXS as a function of minority component volume fraction and temperature. After casting from toluene, samples were

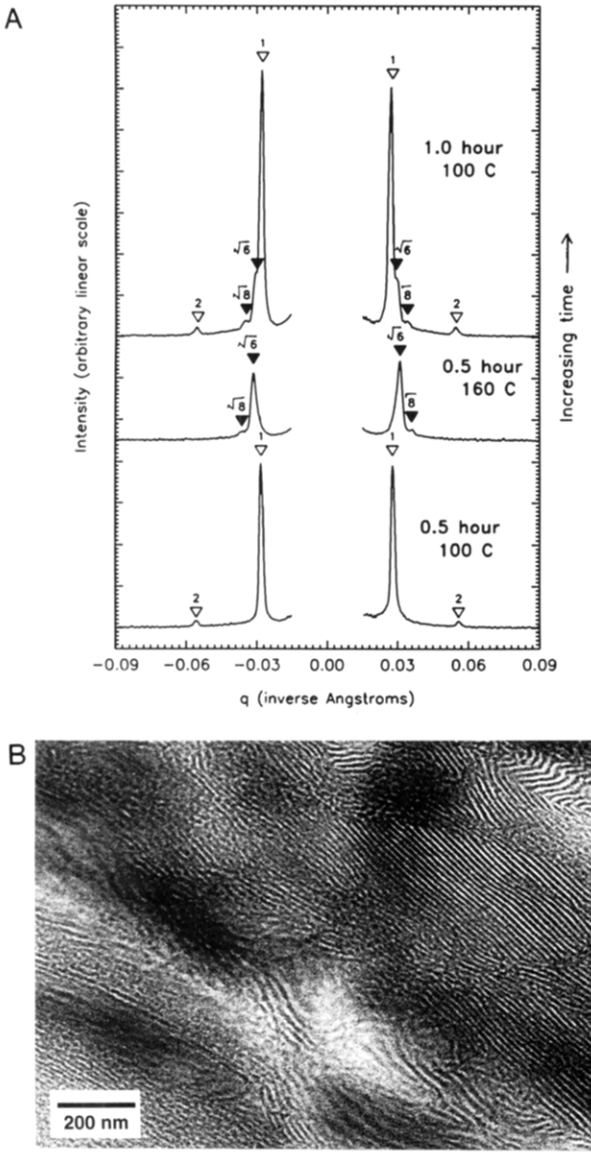

Figure 10. (A) Series of scattering profiles indicating partial thermoreversibility of the L-to-G transition. Peak positions for the original lamellar morphology are indicated with hollow triangles; peak positions for the high-temperature gyroid* morphology are indicated with filled triangles. After casting, annealing the diblock film for 0.5 h at 100 °C produced a lamellar morphology (lower profile). After 0.5 h at 160 °C, diffraction indicated complete conversion of the sample to the gyroid* morphology (middle profile). Subsequent annealing for 1.0 h at 100 °C caused the return of the initial lamellar microstructure, as seen by the reappearance of the lamellar diffraction signature. With further annealing at 100 °C, the intensity of the lamellar peaks increases and the intensity of the gyroid* signature declines. Complete conversion of the sample to the low-temperature lamellar morphology as demonstrated by the disappearance of the gyroid* signature is not observed after annealing periods of up to 20 h at 100 °C, suggesting that the reverse transformation may be kinetically limited. (B) TEM image of a partially thermoreversed gyroid* phase sample. After casting from toluene, the sample was annealed for 0.5 h at 110 °C (initial lamellar microstructure confirmed via SAXS), 1.0 h at 150 °C (total conversion to gyroid* morphology confirmed via SAXS), and 112 h at 110 °C, followed by quenching in liquid nitrogen. Large regions of a chaotic microphase-separated morphology as well as regions showing a layered structure (lower left) predominated in TEM images of this sample, but locally ordered regions of lamellae (upper right) were also observed. This confirms the thermoreversible nature of the lamellar to gyroid* transition.

heated to the appropriate annealing temperature and examined via SAXS after 1 h of *in-situ* annealing (Figure

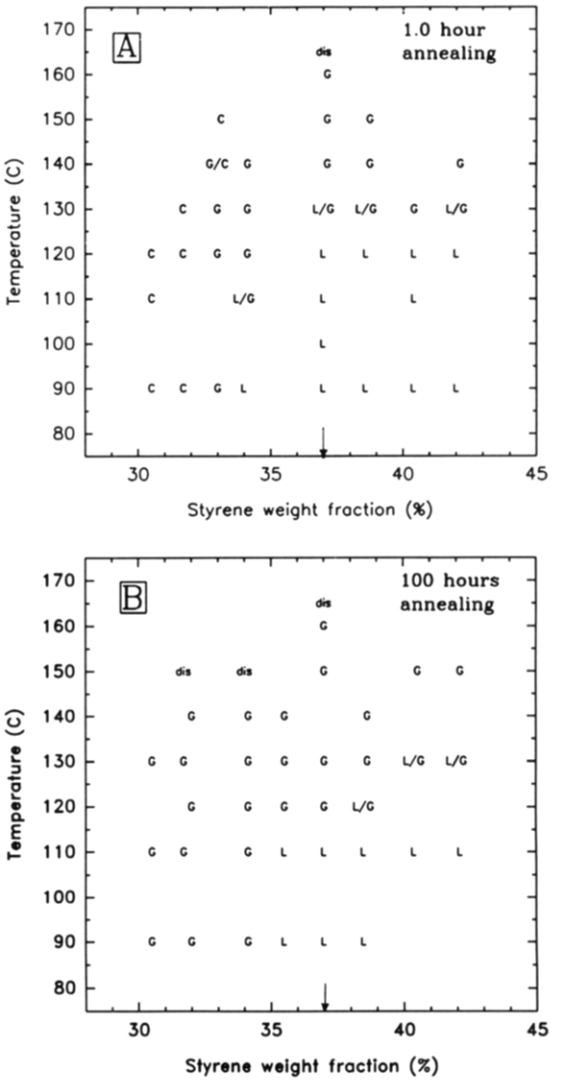

Figure 11. Phase diagrams indicating the observed microphase as a function of temperature and styrene (minority component) weight fraction after 1 h (A) and 100 h (B) of annealing. The pure diblock copolymer has a styrene fraction of 37 wt % and is indicated by an arrow; samples to the left of this mark have been blended with homopolyisoprene, while samples to the right have been blended with homopolystyrene. L denotes the lamellar morphology; G denotes the gyroid*; C denotes hexagonally packed cylinders; and "dis" denotes an isotropic disordered phase. Coexisting morpologies are indicated with a "/" symbol.

11A) or after 100 h of annealing in an oven, followed by quenching in liquid nitrogen and SAXS examination at room temperature (Figure 11B). Previous work on thermoreversible transitions in block copolymers has called attention to the difficulties involved in determining equilibrium microstructure at temperatures where kinetic effects are believed to be significant.[27] Although the addition of a small amount of a low molecular weight homopolymer decreases the relaxation times of the system, kinetic effects may still exert an influence on system behavior. Therefore, we do not claim to have determined the equilibrium microstructure of the blends as a function of temperature. The gyroid* structure appears over limited temperature ranges in samples containing styrene weight fractions from 0.31 to 0.42. It is interesting to note that the OBDD structure, predicted to occur in a band separating the lamellar and cylindrical phases in the strong segregation limit, is not observed. The formation of small numbers of large single-crystal domains (characterized by considerable azimuthal variation in the scattered intensity

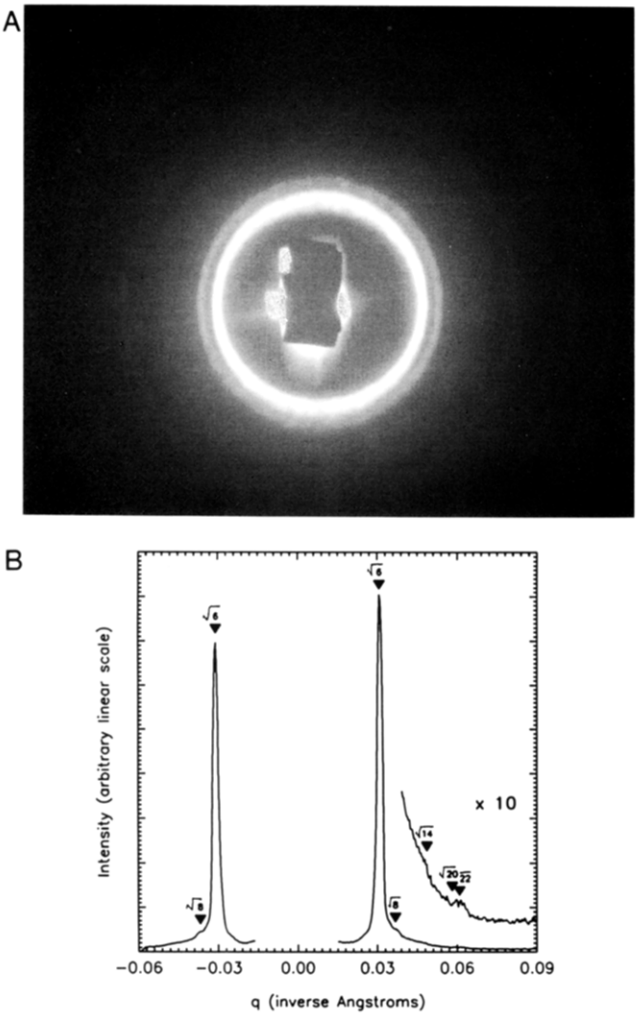

Figure 12. (A) Two-dimensional scattering image obtained from a blend (34 wt % styrene) annealed for 1 h at 135 °C to establish the gyroid* phase, followed by 1 h of annealing at 120 °C before beginning the X-ray exposure. This image was obtained after integrating for 5 h at 120 °C; comparison of diffraction before and after this period revealed no change in the scattering from the sample. (B) One-dimensional profile prepared from the two-dimensional image. $\sqrt{6}$, $\sqrt{8}$, $\sqrt{14}$, $\sqrt{20}$, and $\sqrt{22}$ denote the position ratios of the observed reflections; as discussed in the text, the observation of the $\sqrt{14}$ reflection provides additional evidence for the assignment of $Ia3d$ symmetry.

as shown in Figure 4B) were also observed in blends near the order–disorder transition; such "spotty diffraction" was produced by both gyroid* and cylindrical phase samples.

Attempts to obtain higher diffraction orders from gyroid*-phase blends by following the annealing treatment previously described for the pure diblock copolymer produced higher diffraction peaks in samples containing 34 wt % styrene; see Figure 12. Bragg reflections appear at position ratios of $\sqrt{3}$:$\sqrt{4}$:$\sqrt{7}$:$\sqrt{10}$:$\sqrt{11}$; the appearance of a $\sqrt{7}$ peak indicates that the true spacing ratios are $\sqrt{6}$:$\sqrt{8}$:$\sqrt{14}$:$\sqrt{20}$:$\sqrt{22}$. Although the $\sqrt{14}$ reflection is apparently cancelled by the structure factor of the gyroid* morphology in the pure diblock, cancellation does not occur in this blend due to the different minority component volume fraction.

Discussion

The geometries of the OBDD and gyroid* morphologies resemble one another in several ways; the characteristics of the former structure have been previously discussed in detail by Anderson and Thomas.[28] Both structures consist of a channel-forming minority phase embedded in a matrix formed by the majority component. Minority and majority components are continuous and periodic in all three principal directions. The channels are subdivided into two distinct, interpenetrating networks. In the OBDD, channels in a particular network are tetrahedrally connected; in the gyroid*, the channels join as triads and the two networks are enantiomorphic (mirror images of one another). Underlying the topology of each phase is an infinite triply periodic minimal surface (the D surface for the OBDD, the G surface for the gyroid*) which bisects the matrix phase. Minimal surfaces are two-dimensional constructs embedded in three dimensions which possess zero mean curvature at all points on the surface; the mean curvature at a point is the average of the two principal curvatures. Such structures minimize surface area among all nearby surfaces produced by local perturbations of the initial structure; they were first proposed as possible structural models for bicontinuous fluids by Scriven.[29] Closely related to these minimal surfaces are surfaces of constant (nonzero) mean curvature (CMC surfaces), which minimize area among all nearby surfaces produced by perturbations that preserve the volumes of the regions on either side of the surface. Anderson[19] has discovered families of CMC surfaces for the Schwarz D and P minimal surfaces; recent work by G-Brauckmann and Wohlgemuth[30] suggests that a family of CMC surfaces may exist for the Schoen G minimal surface as well. It is possible, though by no means certain, that the interface separating the two blocks in the OBDD geometry is a CMC surface;[28] a similar result may hold for the gyroid* structure. Thomas et al.[8] have shown that implicit in the thermodynamics of strongly segregated block copolymers are considerations which lead mathematically to the formation of CMC surfaces. It is not immediately obvious that such an approach leads to similar structures in intermediate or weakly segregated systems, where the interface separating the two blocks is quite broad; it is therefore interesting that a bicontinuous cubic structure which may possess constant mean curvature has now been unequivocally observed in a weakly segregated melt.

Measurements of the dimensions of both blocks in the lamellar and gyroid* phases suggest that the transition from the lamellar to the gyroid* structure is driven by a change in chain conformational energy. As the material is in the weak to early intermediate segregation regime over the temperature range of interest, the interfacial width is a significant fraction of the domain thickness. The following estimates of chain dimensions, which assume an infinitely narrow interface across which no mixing of dissimilar chains occurs, are therefore of limited applicability to the experimental situation. However, in the absence of a thorough treatment of interfacial effects, such calculations may suggest why the new cubic morphology is observed.

At 120 °C (for the pure diblock, the temperature at which the initial lamellar structure transforms into the gyroid* over approximately 5 h), the 212 Å repeat spacing for the lamellar structure implies thicknesses of 140 and 72 Å for the isoprene and styrene layers, respectively; the half-layer thicknesses (which measure the elongation of individual chains normal to the lamellar interface) are 70 Å (isoprene) and 36 Å (styrene). The root-mean-square end-to-end distance of a free isoprene chain with M_n = 17 100 is 103 Å[31] at 120 °C, while the corresponding value for a free styrene chain with M_n = 10 300 is 67 Å.[32] Both

chains are therefore compressed, a curious situation since it implies that the total free energy of the system could be reduced by an elongation of the chains perpendicular to the interface involving a corresponding decrease in the interfacial contact area. The reason for the stability of the lamellar phase in this situation is unfortunately unclear. The area per chain junction point, estimated from the molecular weight of the styrene block and the density of polystyrene homopolymer at 120 °C,[32] is 467 Å^2.

For the constant thickness gyroid* structure at 120 °C, the domain dimensions may be estimated from the model, yielding a constant isoprene layer half-thickness of 60 Å and a mean styrene layer half-thickness of 60 Å. The actual half-thickness of the styrene channels ranges from 50 to 80 Å in this model. Note that the polystyrene chains are the more important of the two entropic "springs" in the system since they are of lower molecular weight. The area per chain junction point is 480 Å^2, a difference of less than 3% from the value in the lamellar phase. These values imply that the transition from lamellar to constant-thickness gyroid* is driven by the relaxation of the polystyrene chain; the formation of a slightly curved interface, which this process requires, forces the isoprene chain to expand laterally along the SI interface. This is accomplished with little change in interfacial area due to the curvature of the SI interface and the corresponding distortion of the volumes occupied by single chains from their roughly cylindrical shapes in the lamellar phase. As entropic energies such as chain-conformational terms should dominate the free energy of the system at high temperatures, it may be that the gyroid* structure represents the best minimization of interfacial area that the system can achieve subject to the need to have different domain sizes and a curved interface for the two blocks at high temperatures. Similar considerations have been used to explain the appearance of cubic phases in lipid–water systems.[33]

An alternative model of the gyroid* microstructure assigns the polystyrene domains the structure of a network of appropriately connected cylinders of fixed radius so as to minimize the variation of the domain size of the shorter block. Although such a structure possesses unphysical discontinuities in surface curvature where the cylinders join, an advantage of this "interconnected rod" model is that the deformation of the shorter styrene chains forming the cylinders is believed to be of greater importance than that of the longer isoprene chains forming the matrix. At a styrene volume fraction of 0.33, the interconnected rod model for the gyroid* phase at 120 °C predicts a (constant) radius for the styrene domains of 62 Å, with isoprene domain half-thicknesses ranging from 50 to 80 Å.[34] The interfacial area per chain junction point is estimated to be 486 Å, an increase of 4% from the value obtained for the lamellar phase. Thus, transformation of the lamellar structure to the interconnected rod gyroid* is also driven by the relaxation of the polystyrene chain: indeed, the half-thickness of the styrene domains in the interconnected rod model more closely approaches the equilibrium end-to-end distance expected for styrene homopolymer of the appropriate molecular weight. The experimental data suggest that the S chains in the gyroid* phase are highly relaxed, while the I chains are not: addition of a small amount of short-chain homopolystyrene does not significantly alter phase behavior, while addition of homopolyisoprene causes a noticeable decrease in the lamellar-to-gyroid* transition temperature. In the latter case, the presence of homopolymer may permit the I chain to extend normal to the SI interface (thus assuming a more relaxed configuration) while maintaining both a constant segmental density in the matrix and the interfacial area per block junction required by the relaxed configuration of the S chain.

A third model, currently under investigation, involves the development of a family of constant mean curvature surfaces based on the G surface. The surface area per unit volume (i.e., the surface area at fixed sample composition) will be smallest for the constant mean curvature structure, if such structures exist for the G surface. The constant-thickness structure will be next in area and the interconnected rod structure will have the largest surface area. Depending on the volume fraction of the minority component, mathematical descriptions of the latter two models may possess unphysical discontinuities in surface curvature, but they still may prove useful in developing the geometrical characteristics of the gyroid* morphology. It is important to recognize that the differences in microstructure among the three models considered here (constant thickness, interconnected rod, and constant mean curvature) are very small and may not in fact be resolvable by current experimental data. We are therefore unable to say which microstructure best represents the observed gyroid* phase at the present time. Determination of the appropriate microstructure will require a considerable amount of effort.

Finally, we note that the OBDD family of CMC structures has a deep minimum in the plot of surface area versus volume fraction at a composition of 26.2%.[19,28] The OBDD is experimentally found for compositions ranging from 27% to 33%, suggesting that this bicontinuous phase appears only in systems where it is most efficient (compared to other possible morphologies) in dividing regions while minimizing surface area. If a family of CMC surfaces based on the G surface can be shown to exist, perhaps these structures will also exhibit a deep minimum in this composition range. The factors which determine whether the OBDD or gyroid* morphology will appear in a sample of appropriate composition are at present unknown; it is particularly interesting that the gyroid* morphology appears in this system over the composition range in which the OBDD is observed in similar strongly segregated SI diblock and star block polymers. A recent theoretical treatment of block copolymer microstructure in the weak segregation limit[35] has found a cubic phase of *Ia*3*d* symmetry to be stable in the composition region separating the lamellar and cylindrical morphologies on the phase diagram. Although cubic phases of *Pn*3*m* symmetry were not found to be stable at any composition, the results do not extend to the strong segregation limit where the OBDD were originally observed.[3] Future work, perhaps involving a polymer which exhibits a transition between the gyroid* and OBDD phases as a function of either temperature or composition, may provide insight on this issue.

Conclusions

The existence of a new bicontinuous cubic morphology in intermediate to weakly segregated SI diblock copolymers has now been demonstrated by a combination of SAXS, computer modeling, and TEM. Although scattering data from the new structure is weakly consistent with diffraction from a number of cubic space groups (including *Pn*3*m*, the symmetry of the OBDD morphology), the observed reflections are most consistent with space group *Ia*3*d*. Computer models of a constant-thickness microstructure for the new phase (based on Schoen's G minimal surface

and possessing *Ia3d* symmetry) were used to predict diffraction amplitudes for the new phase; the predicted values agreed better with experimental results than similar calculations performed for the OBDD morphology. TEM images exhibiting 3- and 4-fold rotational symmetry were well matched with simulated images computed from a constant-thickness structure based on the gyroid minimal surface. Power spectra of the experimental images also agreed well with the expected Fourier coefficients based on SAXS.

Acknowledgment. The authors thank Z. Xu and D. Gobran for performing the initial SAXS and TEM on which this work was based, J. Chen for performing the optical measurements and assisting with Fourier transforms of the micrographs, M. Wohlgemuth for useful discussions concerning the gyroid surface, and R. Lescanec for critical evaluation of the manuscript. Work at Princeton University was supported by the U.S. Department of Energy (DE-FG02-87ER60522) and the National Science Foundation (DMR-922-3966); work at M.I.T. was supported by the Air Force Office of Scientific Research (91-0078) and the National Science Foundation (DMR-92-1483).

References and Notes

(1) Schoen, A. H. NASA Technical Report No. 05541, 1970.
(2) Bates, F. S.; Fredrickson, G. H. *Annu. Rev. Phys. Chem.* **1990**, *41*, 525.
(3) Thomas, E. L.; Alward, D. B.; Kinning, D. J.; Martin, D. C.; Handlin, D. L.; Fetters, L. J. *Macromolecules* **1986**, *19*, 2197.
(4) Hasegawa, H.; Tanaka, H.; Yamasaki, K.; Hashimoto, T. *Macromolecules* **1987**, *20*, 1651.
(5) Winey, K. I.; Thomas, E. L.; Fetters, L. J. *Macromolecules* **1992**, *25*, 422.
(6) Spontak, R. J.; Smith, S. D.; Ashraf, A. *Macromolecules* **1993**, *26*, 956.
(7) Olmsted, P. D.; Milner, S. T. *Phys. Rev. Lett.* **1994**, *72*, 936. An improved calculation by these authors suggests that the OBDD is, in contrast to the calculations of ref 7, unstable with regard to the cylindrical morphology in the strong segregation limit (Milner, S. T., personal communication).
(8) Thomas, E. L.; Anderson, D. M.; Henkee, C. S.; Hoffman, D. *Nature* **1988**, *334*, 598.
(9) Disko, M. M.; Liang, K. S.; Behal, S. K.; Roe, R. J.; Jeon, K. J. *Macromolecules* **1993**, *26*, 2983.
(10) Hamley, I. W.; Koppi, K. A.; Rosedale, J. H.; Bates, F. S.; Almdal, K.; Mortensen, K. *Macromolecules* **1993**, *26*, 5959.
(11) Gobran, D. Ph.D. Thesis, University of Massachusetts, Amherst, MA, 1990.
(12) Morton, M.; Fetters, L. J. *Rubber Chem. Technol.* **1975**, *48*, 359.
(13) Hashimoto, T.; Ijichi, Y.; Fetters, L. J. *J. Chem. Phys.* **1988**, *89* (4), 2463.
(14) Lescanec, R. L.; Muthukumar, M. *Macromolecules* **1993**, *26*, 3908.
(15) Tate, M. W.; Eikenberry, E. F.; Gruner, S. M., in preparation.
(16) Gonzales, R. C.; Wintz, P. *Digital Image Processing*; Addison-Wesley: Reading, MA, 1977.
(17) Schwarz, H. A. *Gesammelte Mathematische Abhandlungen*; Springer: Berlin, 1890.
(18) Ström, P.; Anderson, D. M. *Langmuir* **1992**, *8*, 691.
(19) Anderson, D. M.; Davis, H. T.; Scriven, L. E.; Nitsche, J. C. C. *Adv. Chem. Phys.* **1990**, *37*, 337.
(20) Warren, B. E. *X-ray Diffraction*; Addison-Wesley: Reading, MA, 1969.
(21) Harper, P. E. Ph.D. Thesis, Princeton University, Princeton, NJ, 1994, in preparation.
(22) Fontell, K. *Colloid Polym. Sci.* **1990**, *268*, 264.
(23) F. Bates (personal communication) has observed an unusual bicontinuous structure in a weakly segregated SI diblock melt undergoing a shear deformation; although the structure has not been clearly identified, it may also possess *Ia3d* symmetry and represent an independent observation of the structure discussed here. In another report (Schulz, M. F.; Bates, F. S.; Almdal, K.; Mortensen, K. *Phys. Rev. Lett.*, in press), diffraction consistent with the *Ia3d* space group and hence indicative of the gyroid* morphology has been observed from a shear-oriented polystyrene–poly(2-vinylpyridine) diblock copolymer which undergoes a transition from hexagonally packed cylinders to the *Ia3d* morphology with increasing temperature.
(24) Gruner, S. M. *J. Phys. Chem.* **1989**, *93*, 7562.
(25) Winey, K. I.; Thomas, E. L.; Fetters, L. J. *Macromolecules* **1992**, *25*, 2645.
(26) Winey, K. I.; Thomas, E. L.; Fetters, L. J. *J. Chem. Phys.* **1991**, *95*, 9367.
(27) Hajduk, D. A.; Gruner, S. M.; Rangarajan, P.; Register, R. A.; Fetters, L. J.; Honeker, C.; Albalak, R. J.; Thomas, E. L. *Macromolecules* **1994**, *27*, 490.
(28) Anderson, D. M.; Thomas, E. L. *Macromolecules* **1988**, *21*, 3221.
(29) Scriven, L. E. *Nature* **1976**, *263*, 123.
(30) G-Brauckmann, K.; Wohlgemuth, M. Personal communication.
(31) Fetters, L. J. Personal communication (data collected by R. Krishnamoorti).
(32) Boothroyd, A.; Renee, A.; Wignall, G. D. Temperature Coefficients for the Chain Dimensions of Poly(styrene) and Poly(methyl methacrylate). *J. Chem. Phys.*, in press.
(33) Anderson, D. M.; Gruner, S. M.; Leibler, S. *Proc. Natl. Acad. Sci. U.S.A.* **1988**, *85*, 5364.
(34) Gulik, A.; Luzzati, V.; De Rosa, M.; Gambacorta, A. *J. Mol. Biol.* **1985**, *182*, 131.
(35) Matsen, M. W.; Schick, M. *Phys. Rev. Lett.* **1994**, *72*, 2660.
(36) Hahn, T. Ed. *International Tables for X-ray Crystallography*, 3rd ed.; Kluwer Academic Publishers: Boston, MA, 1992; Part A, p 47.